FZJ-IKP(TH)-1999-23

EFFECTIVE FIELD THEORY FOR THE TWO–NUCLEON SYSTEM

Ulf-G. Meißner
FZ Jülich, IKP (Th), D-52425 Jülich, Germany

Abstract

I discuss the dynamics of the two–nucleon system as obtained from a chiral nucleon–nucleon potential. This potential is based on a modified Weinberg power counting and contains chiral one– and two–pion exchange as well as four–nucleon contact interactions. The description of the S–waves is very precise. Higher partial waves are also well reproduced. We also find a good description of most of the deuteron properties.

INTRODUCTION

One of the most important and most intensively studied problems of nuclear physics is deriving the forces between nucleons. While there have been many successful and very precise models (of more or less phenomenological type), only in the last decade the powerful methods of effective field theory (EFT) have been used to study this question. In particular, Weinberg(1) employed power–counting to the irreducible n–nucleon interaction and obtained leading order results by iterating such type of potential in a Lippmann–Schwinger equation. This type of resummation is necessary to deal with the shallow bound states (or large S–wave scattering lengths) present in the two–nucleon system. This is in contrast to conventional chiral perturbation theory in the meson and meson–nucleon sectors, where all interactions can be treated perturbatively. A full numerical study based on Weinberg's approach at next-to-next-to-leading (NNLO) order was performed in ref.(2). It was concluded that the approach could give qualitative insight but was not precise enough to compete with the accurate modern potentials or even phase shift analysis. In addition, a novel power counting scheme was proposed by Kaplan, Savage and Wise (KSW)(3). In that approach, only the leading order momentum–independent four–nucleon interaction is iterated and all other effects, in particular the coupling of pions, are treated perturbatively. This is in stark contrast to Weinberg's scheme, were one–pion exchange (OPE) is present already at leading order and is iterated (among other interactions). What I will show in the following is that a suitably modified Weinberg scheme can be turned into a precision tool, which allows to study systematically the interactions between few nucleons. This lends credit to Weinberg's ideas spelled out almost 10 years ago.

CHIRAL EXPANSION OF THE NN POTENTIAL

EFT is, by construction, only useful in a space of momenta below a certain scale. The latter depends on the system one is investigating. In what follows, I will be concerned with the effective potential between nucleons as defined (and somewhat modified) in ref.(1). In the EFT approach suggested by Weinberg, one has to deal with two different types of interactions. First, there is OPE, two–pion exchange and so on, to describe the long and medium range physics. Second, there are four–nucleon contact interactions to describe the short (and to some extent the medium) range physics. So we have a scale separation, the dividing line being somewhere above twice the pion mass and below the typical scale of chiral symmetry breaking, $\Lambda_\chi \simeq 1\,\mathrm{GeV}$. The problem at hand can be treated exactly by integrating out the pionic degrees of freedom from the Fock space using the projection formalism of Okubo, Fukuda, Sawada and Taketani(4). The usefulness of this approach when applied to momentum space has been demonstrated in a toy–model calculation, see refs.(5). Based on this approach, we have set up the following scheme. First, one constructs the irreducible chiral NN potential based on a power counting in harmony with the projection formalism. This is outlined in detail in ref.(6). To third order in small momenta, this potential is given by the following contributions (LO = leading order, NLO = next-to-leading order):

LO OPE with lowest order insertions and two 4N contact interactions without derivatives.

NLO Vertex and self–energy corrections to the LO interactions, TPE with lowest order insertions and seven 4N contact interactions with two derivatives.

NNLO Vertex and self–energy corrections to OPE as well as TPE with exactly one insertion from the dimension two πN Lagrangian. These terms encode non–trivial information about the pion–nucleon interaction beyond leading order and are thus sensitive to the chiral structure of QCD.

This potential is divergent. All divergences (of quadratic and logarithmic form) can be dealt with by subtracting divergent loop integrals, which leads to an overall renormalization of the axial–vector coupling g_A and seven of the nine coupling constants related to the 4N interactions. The precise prodecure is discussed in detail in ref.(7). The renormalized potential still has a bad high energy behaviour. Some of the contact interactions (NNLO TPE contributions) grow quadratically (cubically) with increasing momenta. Even the momentum–independent contact interactions necessitate regularization, which is performed on the level of the Lippmann–Schwinger equation. That is done in the following way:

$$V(\vec{p},\vec{p}\,') \to f_R(\vec{p})\, V(\vec{p},\vec{p}\,')\, f_R(\vec{p}\,') \;, \tag{1}$$

where $f_R(\vec{p})$ is a regulator function chosen in harmony with the underlying symmetries. In ref.(7), two different regulator functions are used, the sharp cutoff $f_R^{\rm sharp}(\vec{p}) = \theta(\Lambda^2 - p^2)$, and an exponential form, $f_R^{\rm expon}(\vec{p}) = \exp(-p^{2n}/\Lambda^{2n})$, with $n = 2, 3, \ldots$. The latter form is more suitable for the calculation of some observables. Bound and scattering states can then be obtained by solving the Lippmann–Schwinger equation with the regularized potential.

PARAMETERS AND FITTING PROCEDURE

In this section, I briefly describe how the parameters are pinned down. The parameters related to the pion–nucleon interaction beyond leading order can be fixed by a fit of the chiral perturbation theory pion–nucleon amplitude(8) to the dispersion–theoretical one inside the Mandelstam triangle(9). In addition, we have nine coupling constants related to four–nucleon contact interactions. These can be uniquely determined by a fit to the S– and P–waves together with the mixing parameter ϵ_1. While both S–waves contain two parameters, the P–waves and ϵ_1 depend one (more precisely, one can form linear combinations of the LECs which appear as these parameters in the considered partial waves). At NLO, the resulting values for the LECs related to the 4N contact terms are sensitive to the energy range used in the fit. At NNLO, the resulting values are more stable, so that we can perform global fits for energies up 100 MeV. For example, such a global fit with $\Lambda = 500$ MeV at NLO and 875 MeV at NNLO leads to a deuteron binding energy of $E_d = -2.17$ and -2.21 MeV at NLO and NNLO, respectively. Therefore, without any fine tuning, we can reproduce the empirical value within 2 percent and 1 permille at NLO and NNLO, in order. The increase of the cut–off value when going from NLO to NNLO is related to the fact that at NNLO, the chiral TPEP includes mass scales above the two–pion mass, which is the scale related to the uncorrelated TPEP appearing at NLO. It is also worth mentioning that the quality of the fits increases visibly as one goes from LO to NLO to NLO (for details, see ref.(7)). This is, of course, expected from the underlying power counting. With that, one can predict these partial waves for energies above 100 MeV. All other partial waves with angular momentum ≥ 2 and the deuteron properties are *predictions*.

Prediction for the S– and P–waves

The resulting S–waves are shown in figs.1,2 in comparison to the Nijmegen phase shift analysis (PSA)(10). The improvement when going from LO to NLO to NNLO is clealy visible.

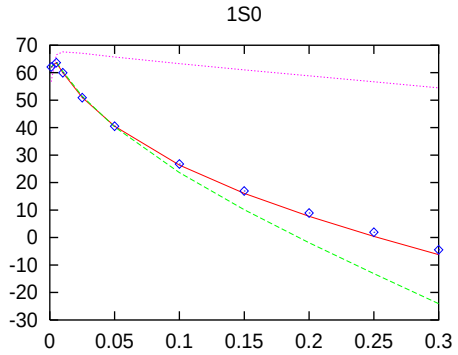

Fig. 1. Predictions for the ${}^1S_0$ partial wave (in degrees) at LO (purple curve), NLO (green curve) and NNLO (red curve) in comparison to the Nijmegen PSA (blue diamonds) for nucleon laboratory energies up to 0.3 GeV.

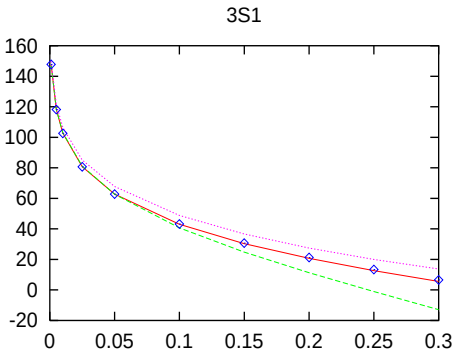

Fig. 2. Predictions for the ${}^3S_1$ partial wave (in degrees) at LO (purple curve), g NLO (green curve) and NNLO (red curve) in comparison to the Nijmegen PSA (blue diamonds) for nucleon laboratory energies up to 0.3 GeV.

The P–waves are mostly well described, although the NNLO TPEP is a bit too strong in ${}^3P_1$ and ${}^3P_2$. Of particular interest is ϵ_1 since it has also been calculated at NLO(3) and NNLO(12) in the KSW approach. Our results (note that we used the so–called Stapp parametrization(13) for the coupled triplet waves) are shown in comparison to the ones of refs.(3,12) in fig.3 as a function of nucleon cms momentum up to 350 MeV. For energies below 150 MeV, the KSW results are comparable to ours, but is obvious from that figure that their approach is tailored to work at low energies. If one wants to go to momenta above 100 MeV, it appears that pion exchange should be treated non–perturbatively.

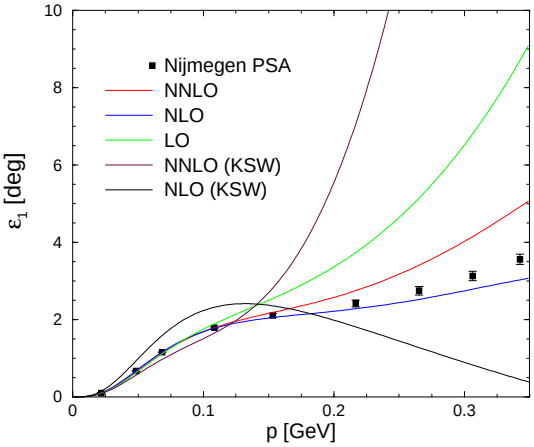

Fig. 3. The ${}^3S_1 - {}^3D_1$ mixing parameter ϵ_1 for our approach and the KSW scheme in comparison to the Nijmegen PSA as a function of the nucleon cms momentum.

I also would like to discuss briefly the so–called effective range expansion. For any partial

wave, one can write

$$p\,\cot\delta = -\frac{1}{a} + \frac{1}{2}\,r\,p^2 + v_2\,p^4 + v_3\,p^6 + \mathcal{O}(p^8)\ , \tag{2}$$

with δ the phase shift, p the nucleon cms momentum, a the scattering length and r the effective range. It has been stressed in ref.(11) that the shape parameters v_i are a good testing ground for the range of applicability of the underlying EFT. At NNLO, we find e.g. $a = 5.424\,(5.420)\,\mathrm{fm}$, $r = 1.741\ (1.753)\,\mathrm{fm}$, $v_2 = 0.046\ (0.040)\,\mathrm{fm}^3$, and $v_3 = 0.67\ (0.67)\,\mathrm{fm}^5$ for ${}^3S_1$. Similarly, for ${}^1S_0$, we have $a = -23.72\,(-23.74)\,\mathrm{fm}$, $r = 2.68\ (2.67)\,\mathrm{fm}$, $v_2 = -0.61\ (-0.48)\,\mathrm{fm}^3$, and $v_3 = 5.1\ (4.0)\,\mathrm{fm}^5$. The numbers in the square brackets refer to the np system from the Nijmegen II potential . Note that one can also perform the fit such that the scattering lenghts and effective ranges are exactly reproduced. This leads only to modest changes in the values of $v_{2,3}$, e.g. for such a fit in ${}^1S_0$ one has $v_2 = -0.53\,\mathrm{fm}^3$ and $v_3 = 5.0\,\mathrm{fm}^5$. This rather good agreement illustrates again that the long range physics associated with pion exchanges is incorporated correctly and it demonstrates the predictive power of such an EFT approach.

Predictions for higher partial waves

Consider first the D– and F–waves. These are free of parameters and most problematic since the NNLO TPEP can be too strong. In some potential models, TPEP is simply cut at distances of (approximately) less than one fermi. Nevertheless, we find a rather satisfactory description of these partial waves. Of particular interest is ${}^3D_1$ since it is related to the deuteron channel. Also, ${}^1D_2$ is supposedly very sensitive to contributions from the Δ–resonance, which in our approach is subsumed in the LECs related to the dimension two πN interaction. Both these partial waves are well described, see figs.4,5. Even the small ${}^3D_3$ partial wave is very well described up to the opening of the pion production threshold (in the Bonn potential, this partial wave is dominated by correlated TPE). Note, however, that the D–waves are very sensitive to the choice of the regulator cut–off.

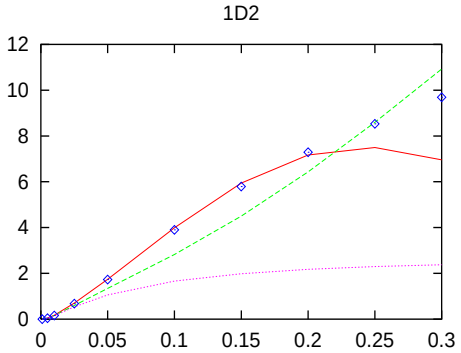

Fig. 4. Predictions for the ${}^1D_2$ partial wave (in degrees) at LO (purple curve), NLO (green curve) and NNLO (red curve) in comparison to the Nijmegen PSA (blue diamonds) for nucleon laboratory energies up to 0.3 GeV.

The so–called peripheral waves ($l \geq 4$) have already been considered by the Munich group(14). Their calculation was based on Feynman graphs using dimensional regularization. The potential was constructed perturbatively by proper partial wave projection of the NNLO OPE and TPE. While in most of the peripheral waves OPE is dominant, there are a few exceptions where chiral NNLO TPEP is needed to bring the predictions in agreement with the data or PSA results. Our calculation, which is based on a completely different regularization scheme and treats the potential non–perturbatively, leads to the same results. This is rather gratyfying. One particular example that demonstrates the importance of NNLO TPEP is ${}^3G_5$ as shown in fig.6.

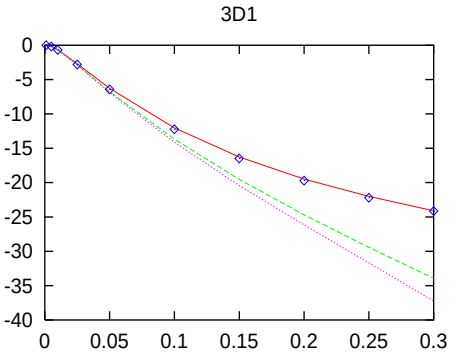

Fig. 5. Predictions for the ${}^3D_1$ partial wave (in degrees) at LO (purple curve), g NLO (green curve) and NNLO (red curve) in comparison to the Nijmegen PSA (blue diamonds) for nucleon laboratory energies up to 0.3 GeV.

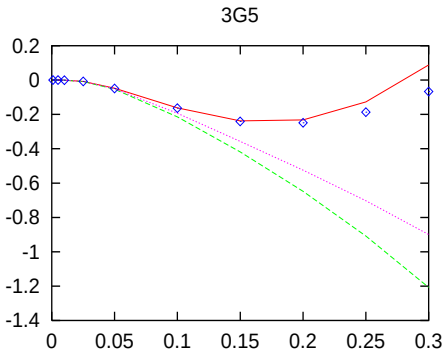

Fig. 6. Predictions for the ${}^3G_5$ partial wave (in degrees) at LO (purple curve), NLO (green curve) and NNLO (red curve) in comparison to the Nijmegen PSA (blue diamonds) for nucleon laboratory energies up to 0.3 GeV.

Deuteron properties

It is straightforward to calculate the bound state properties. At NNLO (NLO), we use an exponential regulator with $\Lambda = 1.05\,(0.60)$ GeV, which reproduces the deuteron binding energy within an accuracy of about one third of a permille (2.7 percent). No attempt is made to reproduce this number with better precision. In table 1 the deuteron properties are collected and compared to the data and two realistic potential model predictions. We note that deviation

Table 1. Deuteron properties derived from our chiral potential compared to two "realistic" potentials (Nijmegen–93(15) and CD–Bonn(16)) and the data. Here, r_d is the root–mean–square matter radius. An exponential regulator with $\Lambda = 600$ MeV and $\Lambda = 1.05$ GeV at NLO and NNLO, in order, is used.

	NLO	NNLO	Nijm93	CD-Bonn	Exp.
E_d [MeV]	2.1650	2.2239	2.224575	2.224575	2.224575(9)
Q_d [fm^2]	0.266	0.261	0.271	0.270	0.2859(3)
η	0.025	0.025	0.0252	0.0255	0.0256(4)
r_d [fm]	1.975	1.967	1.968	1.966	1.9671(6)
A_S [fm$^{-1/2}$]	0.866	0.887	0.8845	0.8845	0.8846(16)
P_D[%]	3.8	6.5	5.67	4.83	–

of our prediction for the quadrupole moment compared to the empirical value slightly larger

than for the realistic potentials. Still, it remains to be checked whether this problem persists when one includes the meson–exchange currents (compare also the discussion in ref.(17)). The asymptotic D/S ratio, called η, and the strength of the asymptotic wave function, A_S, are well described. The D–state probability, which is not an observable, is most sensitive to small variations in the cut–off. At NLO, it is comparable and at NNLO somewhat larger than obtained in the CD-Bonn or the Nijmegen-93 potential. This increased value of P_D is related to the strong NNLO TPEP. At N^{3}LO, I expect this to be compensated by dimension four counterterms. It is also worth mentioning that at NNLO, we have two additional very deeply bound states. These have, however, no influence on the low–energy physics and can be projected out. Furthermore, these states are an artefact of the too strong potential and will most probably vanish at N^{3}LO. Altogether, the description of the deuteron as compared to ref.(2) is clearly improved.

COORDINATE SPACE REPRESENTATION

It is also illustrative to consider the coordinate space representation of this potential. I point out that it is intrinsically non–local in momentum as well as in coordinate space. Therefore, it cannot be directly compared to standard local NN potentials. In fig.7, the corresponding potential in the $^1S_0$ partial wave at NLO is shown. Qualitatively, it exhibits all expected features, namely the short–range repulsion, intermediate range attraction and dominance of pion exchange at large separations (as much as this can be seen in a pictorial of a non–local potential). In ref.(7), a more detailed comparison of the chiral potential with the so–called realistic potentials is given.

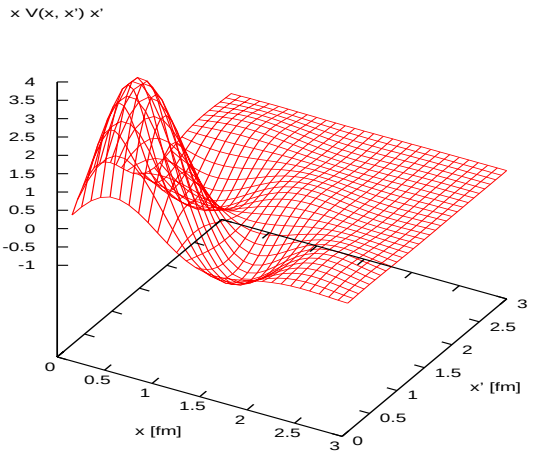

Fig. 7. Coordinate space representation of the potential $xV(x,x')x'$ in the the $^1S_0$ partial wave at NLO.

SUMMARY AND OUTLOOK

In this talk, I have shown some results for the nucleon–nucleon interaction based on effective field theory. The formalism is an extension of the ideas spelled out by Weinberg almost a decade ago. The power counting is performed on the level of the potential. We have worked out the potential to next-to-next-to-leading order in the power counting. At NNLO, it consists of one– and two–pion exchange diagrams with insertions from the dimension one and two pion–nucleon Lagrangian. The corresponding low–energy constants from $\mathcal{L}^{(2)}_{\pi N}$ have been determined from a fit ot the πN amplitudes inside the Mandelstam triangle(9). In addition, there are two/seven four–nucleon contact interactions with zero/two derivatives. The

so–defined potential is divergent. All these divergences can be absorbed by a proper redefinition of the axial–vector coupling g_A and of seven of the nine four–nucleon couplings. This renormalized potential needs to be regularized due to its bad high momentum behaviour, see eq.(1). The regularized potential is used in a Lippmann–Schwinger equation to obtain bound and scattering states by menas of standard Gauss–Legendre quadrature. The corresponding coupling constants can be obtained after proper partial wave decomposition from a fit of the two S– and four P–waves as well as the $^3S_1 - ^3D_1$ mixing parameter ϵ_1 for nucleon lab energies below 100 MeV. The resulting S–waves are as accurate as obtained from high precision potentials (for energies up to the pion production threshold). The other partial waves are mostly well described. For angular momentum ≥ 2, all phase shifts are parameter free predictions. In particular, the $^3D_1$ wave is well reproduced. In some of the D– and F–waves, the NNLO TPEP is somewhat too strong. This will be cured at N^{3}LO due to the appearance of 4N contact interactions with four derivatives. Their contribution is expected to balance the short distance contribution from the TPEP. In most peripheral waves ($l \geq 4$), OPE is dominant but there are some exceptions where NNLO TPE is needed to close the gap between the EFT prediction and the data (or PSA). This has been already found before in refs.(14,18) based on completely different approaches. In addition, without any fine tuning we obtain good results for the deuteron, the sole exception being the too low quadrupole moment. However, it is mandatory to calculate the pertinent exchange currents before drawing a conclusion on this issue. In fact, the EFT approach can easily be extended to the coupling of external fields as well as to systems with more than two nucleons. It is my opinion that the chiral Lagrangian approach does more than "... justify approximations (such as assuming the dominance of two–body interactions) that have been used for many years by nuclear physicists..."(19).

ACKNOWLEDGEMENTS

I am grateful to Evgeny Epelbaum and Walter Glöckle for a most enjoyable collaboration and allowing me to present these results before publication. I would like to thank Iain Stewart for supplying me with the results for ϵ_1 in the KSW scheme and Vincent Stoks for providing the range parameters. Last but not least the superbe organization by Christine Kunz and Res Badertscher is warmly acknowledged.

REFERENCES

1. S. Weinberg, Phys. Lett. **B251**, 288 (1990); Nucl. Phys. **B363**, 3 (1991).
2. C. Ordóñez, L. Ray and U. van Kolck, Phys. Rev. **C53** (1996) 2086.
3. D.B. Kaplan, M.J. Savage and M.B. Wise, Nucl. Phys. **B534**, 329 (1998).
4. S. Okubo, Prog. Theor. Phys. **12**, 603 (1954); N. Fukuda, K. Sawada and M. Taketani, Prog. Theor. Phys. **12**, 156 (1954).
5. E. Epelbaoum, W. Glöckle, and Ulf-G. Meißner, Phys. Lett. **B439**, 1 (1998); E. Epelbaoum, W. Glöckle, A. Krüger and Ulf-G. Meißner, Nucl. Phys. **A645**, 413 (1999).
6. E. Epelbaoum, W. Glöckle and Ulf-G. Meißner, Nucl. Phys. **A637**, 107 (1998).
7. E. Epelbaum, W. Glöckle and Ulf-G. Meißner, in preparation.
8. N. Fettes, Ulf-G. Meißner and S. Steininger, Nucl. Phys. **A640**, 199 (1998).
9. P. Büttiker and Ulf-G. Meißner, `hep-ph/9908247`; Paul Büttiker, *these proceedings*.
10. V.G.J. Stoks et al., Phys. Rev. **C48**, 792 (1993).
11. T.D. Cohen and J.M. Hansen, Phys. Rev. **C59**, 13 (1999).
12. S. Fleming, T. Mehen and I.W. Stewart, `nucl-th/9906056`.
13. H.P. Stapp, T.J. Ypsilantis and N. Metropolis, Phys. Rev. **105**, 301 (1957).
14. N. Kaiser, R. Brockmann and W. Weise, Nucl. Phys. **A625**, 758 (1997).
15. V.G.J. Stoks et al., Phys. Rev. **C49**, 2950 (1994).
16. R. Machleidt, F. Sammarruca and Y. Song, Phys. Rev. **C53**, R1483 (1996).
17. R.B. Wiringa et al., Phys. Rev. **C51**, 38 (1995).
18. M.R. Robilotta and C.A. da Rocha, Nucl. Phys. **A615**, 391 (1997).
19. S. Weinberg, AIP Conference Proceedings **272**, 346 (1993).